Observation of a vortex-glass phase in polycrystalline $YBa_2Cu_3O_{7-x}$ in a magnetic field

T. K. Worthington, E. Olsson, C. S. Nichols,* T. M. Shaw, and D. R. Clarke†
IBM Research Division, IBM Thomas J. Watson Research Center, Yorktown Heights, New York 10598
(Received 19 November 1990)

We report the results of temperature- and field-dependent transport measurements on sintered, polycrystalline samples of $YBa_2Cu_3O_{7-x}$. A study of the E-J curves indicates a second-order phase transition, at low current density in the coupling of the grains, that exhibits the scaling behavior predicted for a vortex glass. The ohmic resistance at low current is observed to vanish at a nonzero temperature, and the E-J curves exhibit power-law behavior at that temperature. Below this temperature the E-J curves are consistent with a true critical current with zero linear resistance. The qualitative features of the data and the values of the critical exponents are consistent with the predictions of the vortex-glass theory. Our findings cannot be explained by the predictions of conventional flux-creep models.

INTRODUCTION

The vision of applications has motivated an enormous number of papers concerning critical currents in polycrystalline high-T_c superconductors. This paper addresses a more basic question: Are high-T_c polycrystalline superconductors really superconducting in magnetic fields above H_{c1}? What do we mean by superconducting? Any real sample will have a nonzero resistivity, $\rho = E/J$, where E is the electric field and J the current density, although the resistance may be immeasurably small. For this paper, we will chose the existence of zero ohmic resistance, $\lim_{J\to 0} E/J = 0$, at a finite temperature as the *sine qua non* of a superconducting phase. There is little question that this definition is met in conventional and high-T_c superconductors when the applied magnetic field is below $H_{c1}(T)$. However, the question is not so clear when the applied field penetrates the material in the Abrikosov or mixed state. Anderson[1] and Kim, Hempstead, and Strand[2] observed and explained the logarithmic decay of persistent currents using a model of thermally activated motion of flux lines out of pinning sites. The Anderson-Kim flux-creep model also predicts that there should be an ohmic resistance at all nonzero temperatures due to the thermal activation of the flux lines out of the pinning wells. This resistance is proportional to $e^{-U/kT}$ where U is the effective pinning well depth. Although the resistance of commercial type-II superconductors can be exceedingly small as is evidenced by the existence of persistent magnets with very long decay times, this prediction implies that in the presence of a penetrating magnetic field, type-II superconductors are not truly superconducting. The Anderson-Kim model has been very successful in explaining the decay of persistent currents[3] in experiments where the current density is at or close to the critical current density, but somewhat less successful in explaining E-J transport data at low current density[4] in samples carefully prepared to have very low pinning. With the development of commercial material with strong flux pinning and large observed critical currents the question became moot. However, since the discovery of materials exhibiting superconductivity at much higher temperatures and with low critical currents the question has resurfaced.[5]

Shortly after the discovery of high-T_c superconductivity, Müller, Takashige, and Bednorz[6] first observed the decay of the magnetization in La_2CuO_{4-y}:Ba polycrystalline samples and the existence of a line in the H-T plane below which the magnetic properties became irreversible. They attributed this behavior to a superconducting glass state first proposed by Ebner and Stroud[7] made up of Josephson coupled grains. It was tempting to associate the granular nature of the polycrystalline samples with these Josephson coupled grains; however, a scaling argument[6] suggested that the coupling was taking place within the physical grains. Worthington *et al.*[8] observed logarithmic decay in the magnetization in single-crystal $YBa_2Cu_3O_{7-x}$ and suggested that this could be explained by traditional Anderson-Kim flux creep. A great number of papers have been published describing the decay of magnetization in both polycrystalline, crystalline, and thin film samples in terms of both the superconducting glass model and in terms of conventional flux creep.[9] In addition there has been a great deal of recent work proposing a variety of models to explain the transport and magnetic properties of high-T_c superconductors in terms of extensions to the traditional flux-creep model, including distributions of barriers,[10] particular shaped barriers,[11] collective pinning,[12] and the possibility of flux liquid phases that might support a critical current.[13]

Recently Fisher[14] proposed that a true superconducting phase might exist in the presence of a penetrating magnetic field in bulk samples with random disorder. Fisher's vortex-glass model differs from the traditional models by considering the vortices as line objects and predicts a second-order phase transition at finite temperature, $T_g(H)$, to a phase which exhibits superconductivity as defined above. There has been recent convincing experimental evidence for the existence of this vortex-glass phase in epitaxial films of $YBa_2Cu_3O_{7-x}$ (Ref. 14) and in

single-crystal $YBa_2Cu_3O_{7-x}$.[16]

Polycrystalline samples are more complicated. In the presence of a penetrating magnetic field, local superconductivity develops within the individual grains at a temperature above the temperature where Josephson coupling between the grains develops. If the sample is cooled in constant applied magnetic field, when the grains become superconducting, flux is forced into the grain boundary regions. It has been assumed that this flux moves in a flux-flow or flux-creep fashion and causes dissipation. However, in this paper we report transport data that support the conclusion that in polycrystalline samples at high field, there is a global superconducting transition at lower temperature where the intergranular vortices become frozen. We will show that these data are in close agreement with the predictions of the vortex-glass model and support the conclusion that polycrystalline high-T_c materials are *real* superconductors even in high magnetic fields.

MATERIALS PREPARATION

The $YBa_2Cu_3O_{7-x}$ materials we have studied were prepared by prereacting powders of $BaCO_3$, Y_2O_3, and CuO at 930 °C in flowing oxygen. The reacted mixtures were ground in a mortar and subsequently milled to a fine powder (~ 3 μm particle size) using a gas jet mill. Pellets were isostatically cold pressed and sintered at 950 °C in pure, dried oxygen after a heating cycle designed to minimize carbon retention.[17] Sample B was given a heat treatment at 970 °C for 5 h before the 950 °C cycle to increase the grain size. The density of the sintered pellets was 81% for sample A and 92% for sample B. The ~ 1.6-cm-diam pellets were sliced into disks that were carefully sawed into the serpentine pattern shown in Fig. 1. Each sample was subsequently ground to ~ 0.3 mm thickness. Gold contacts were sputtered onto the surface and the sample was annealed at 600 °C for 1 h to improve the contact resistance and then at 400 °C for 16 h in 1 atm of flowing O_2 to establish the oxygen content. The serpentine shape of the sample allowed for a substantial increase in electric field sensitivity while maintaining a large cross-sectional area, ~ 0.3 mm^2. The large cross section ensures that the transport results represent the three-dimensional behavior of many grains.

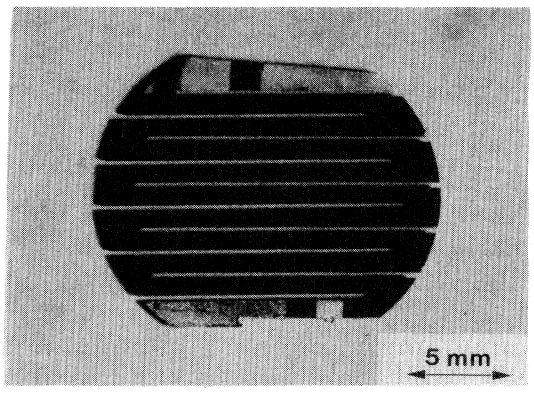

FIG. 1. A photograph showing the serpentine pattern used to achieve large electric field sensitivity.

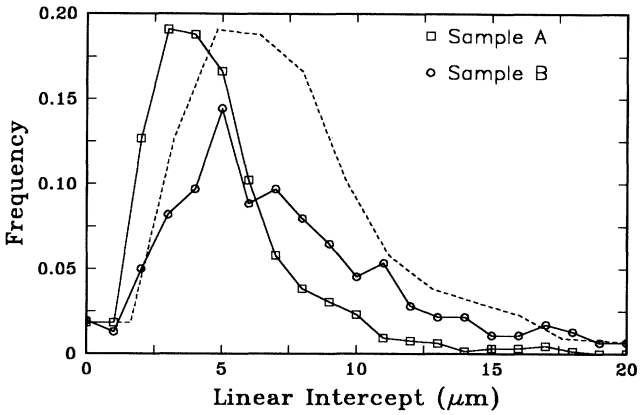

FIG. 2. Histograms of the grain size as measured by linear intercept. Sample A is shown as squares and sample B by circles. The dotted line is the data for sample A scaled by the ratio of the average grain size ($\frac{8}{5}$).

The grain size distributions were characterized by measuring the average linear intercept between grain boundaries. Histograms of the distributions of linear intercepts are shown for both samples in Fig. 2. The average intercept length for sample A was 5 μm and for sample B was 8 μm. Although it is clear from the histograms that sample B has larger grains, because of the skew apparent in these distributions, it is not clear that the average linear intercept length is the most appropriate length to characterize the microstructure. To support the use of this measure, we have plotted the data for sample A multiplied by $\frac{8}{5}$ as the dotted line in Fig. 2. The observation that this constructed histogram has a similar peak location and skew to sample B provides support for our use of the average linear intercept length as the characteristic length to describe the microstructure. These histograms are the sum of several sets of measurements from different regions in the samples. There is no indication of inhomogeneity on length scales larger than the grain size.

TRANSPORT MEASUREMENTS

The transport properties of these samples were studied in a very conventional manner, but as much lower current density than others have used. A constant current was applied using a Keithley 220 current source and the voltage measured with a Keithley 181 nanovoltmeter. Because of the long current path, the system noise level, ~ 20 nV, corresponded to an electric field sensitivity of $\sim 3 \times 10^{-7}$ V/m. The data were taken in constant field for numerous descending temperatures. For each point the voltage was measured for equal positive and negative currents. Figure 3(a) shows the *E-J* curves at 0.3 T for 26 temperatures 1 K apart for sample A.

Figure 3(b) shows the same data plotted as resistivity (E/J) versus J. Figures 4(a) and 4(b) show data for sample B at 1.5 T. Data were taken at other fields and exhibit similar behavior.

An examination of the E-J curves [Figs. 3(a) and 4(a)] indicates that there is a temperature below which the ohmic regime vanishes and downward curvature is evident at all currents. For all the fields for both samples, the E-J curve that separates these regimes were selected. This fixed the glass transition temperature and for the rest of the analysis this value is used. The slope of this curve was measured and found to be 2.7 ± 0.2 for sample A and 2.8 ± 0.2 for sample B. No systematic magnetic field dependence of the slope of the E-J curve at the glass transition temperature was observed. Figure 5 shows the temperature dependence of $T_g(H)$ for the two samples and the temperature where the grains become locally superconducting as measured by ac susceptibility.

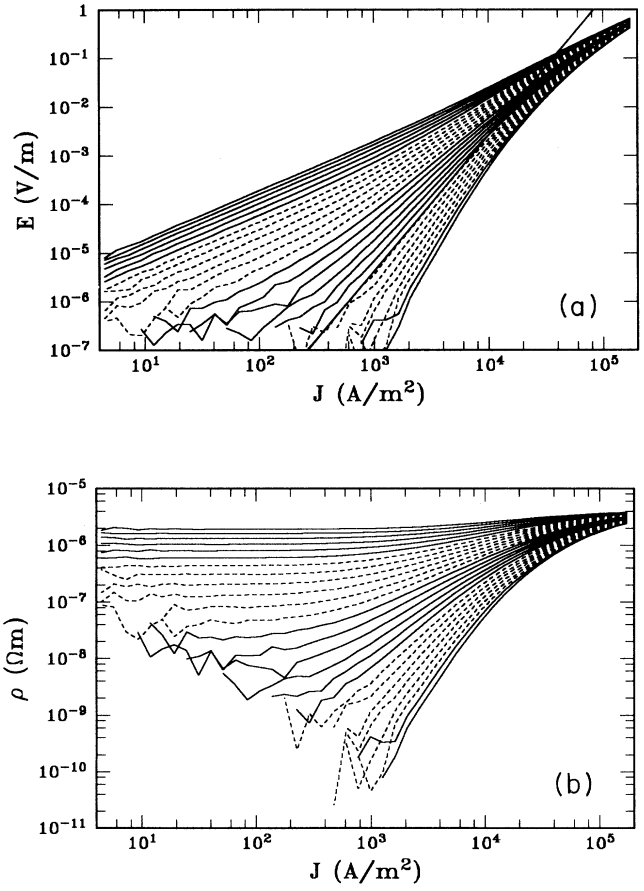

FIG. 3. (a) E-J data for sample A at an applied field of 0.3 T, perpendicular to the current. There are 26 curves at 1 K intervals from 80 to 55 K. The added line at the glass temperature, 62 K, has a slope of 2.8. (b) The same data plotted as resistivity E/J vs J.

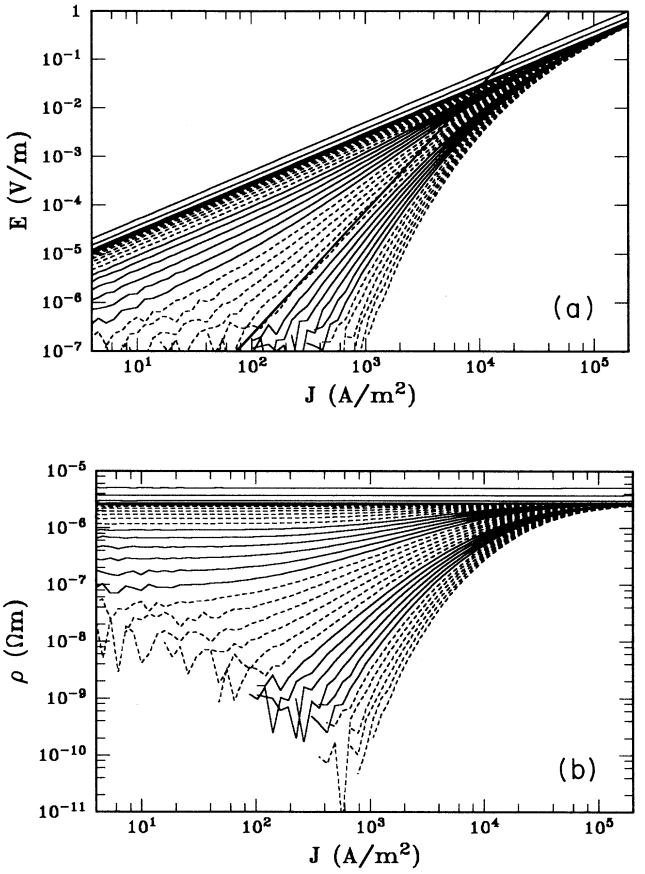

FIG. 4. (a) E-J data for sample B at an applied field of 1.5 T, perpendicular to the current. There are 36 curves at 1 K intervals from 90 to 55 K. The added line at the glass temperature, 67 K, has a slope of 2.6. (b) The same data plotted as resistivity E/J vs J.

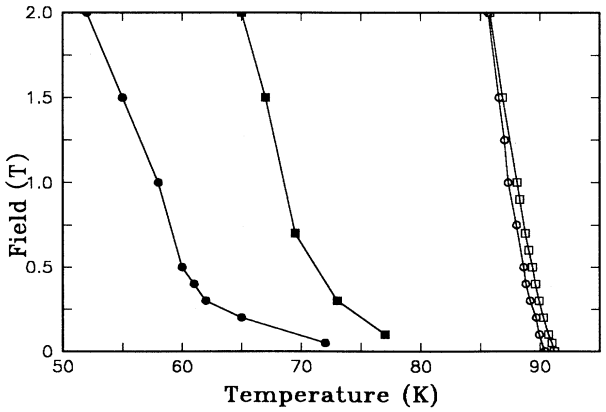

FIG. 5. The values of $T_g(H)$ for sample A (solid circles) and sample B (solid squares). The glass transition of the grains as measured by ac susceptibility is shown as open symbols.

DISCUSSION

The E-J characteristics of polycrystalline superconductors[18] have often been interpreted using phenomenological models based on flux-flow and flux-creep–flux-flow crossover behavior. All of these analyses have been carried out in the strongly nonlinear portion of the E-J curves, above the region where it was implicitly assumed that current independent flux creep occurred. However, as pointed out by Yeshurun and Malozemoff[19] and Tinkham,[20] because of the unprecedented high temperatures and the short coherence length, flux-creep effects, which were not observable in most low-T_c systems, would become significant for the high-T_c materials. As mentioned above, this paper concerns the low current portion of the E-J curves where the behavior is dominated by the interaction of the vortices with the thermal fluctuations. The standard form of the flux-creep model[1,2] predicts a resistivity which is given by

$$\rho=(2\nu BL/J)e^{-U/kT}\sinh(JBV_cL_p/kT) . \quad (1)$$

At low current, the hyperbolic sine term can be replaced by its argument and this leads to a current independent resistivity at low current which has a temperature dependence proportional to $e^{-U/kT}$. Since $\Delta T/T \ll 1$ there is little difference in the data plotted as T or $1/T$ so the prediction of flux creep is that Figs. 3(b) and 4(b) should show equally spaced horizontal lines at low current. Clearly our data are at variance with this prediction.

A number of modifications to the standard flux-creep model have been proposed to explain deviations observed in experiments. One model[11] assumes a particular shape for the current dependence of the pinning wells to explain the E-J behavior at high current density in epitaxial films. However, far from T_c, where the potential well depth is not expected to have a strong temperature dependence, this model predicts that there is a current independent resistivity that does not vanish except at $T=0$. The same is true for models that modify the standard flux-creep model by adding a distribution of barriers.[10] By choosing particular shapes of the barrier distribution, these models can explain power-law E-J behavior, however, they are unable to account for the continuous downward curvature evident at temperatures below T_g.

In striking contrast to these models which predict a slow crossover-type behavior, the vortex-glass model[14] predicts a second-order phase transition at $T_g(H)>0$. Central to this model is the recognition that the vortices are line objects and that they must move over macroscopic distances in order for dissipation to occur. The motion of the vortices which leads to dissipation can be thought of as the growth of vortex loops nucleated by thermal fluctuations. If the fluctuation is large enough, the loop grows due to the force provided by the interaction of the vortex and the current. This growth is impeded by the energy due to the line tension and the interaction of the vortex loop with the random distribution of pinning sites.

Near the transition into the vortex-glass phase, where the vortex-glass correlation length ξ_{VG} is larger than other relevant lengths, e.g., the grain size, an estimate of the current density range where scaling behavior is expected can be made by comparing the thermal energy kT with the energy due to the current density J, of a loop of size L_J,

$$KT=\phi_0 JL_J^2 , \quad (2)$$

where ϕ_0 is the flux quantum. When L_J is larger than any other relevant length in the sample, the physics should be dominated by the fluctuations and the model should describe the transport behavior. For films, this length is approximately the distance between the vortices,[15] indicating that there is very strong disorder. In crystals,[16] the estimate is 15 μm, consistent with the observation that the crystals are much less disordered and have lower critical current. The length scale for intergranular currents in polycrystalline samples is set by the grain size; at lengths longer than the grain size, the sample appears homogeneous.

There are three predictions of the vortex-glass model that can be compared with these transport data.[14]

1. At the phase transition temperature, the E-J data should show a power-law behavior, $E \propto J^{(z+1)/2}$, where the critical exponent z is expected to be in the range of 4–6.

2. Above $T_g(H)$, there should be an ohmic region in the resistivity at low current. The resistivity in this region should vanish at $T_g(H)$ as $\rho \propto t^{\nu(z-1)}$, where $t \equiv |T-T_g|/T_g$. The critical exponent ν is expected to be in the range 1–2.

3. Below $T_g(H)$, the voltage should vanish exponentially in the current, $E \propto e^{-(J_t/J)^{\mu}}$, where the characteristic current J_t should increase below the phase transition as $t^{2\nu}$, and the vortex-glass exponent μ is expected to be in the range 0–1.

We have analyzed our data in the context of this model. The observation of power-law behavior only at a single temperature, with a magnetic field and sample-independent exponent is support for point 1 above. Our value of the critical exponent z, 4.6±0.2 is in good agreement with the data of Koch *et al.*[15] who report a z of 4.8, and Gammel, Schneemeyer, and Bishop[16] who report a z of 4.3±1.5. Above $T_g(H)$ there is a clear ohmic regime, most easily seen in Figs. 3(b) and 4(b). Figure 6(a) shows the ohmic resistance versus $(T-T_g)/T_g$ for sample A at $H=0.05$ T. When plotted as a function of $(T-T_g)/T_g$ all the fields for both samples show identical behavior. Figure 6(b) shows ρ/ρ_0 versus $(T-T_g)/T_g$ for several fields for both samples. The value of $\rho_0(H)$ was chosen to collapse the data. The slope of these data is 3.9±0.2 for small values of reduced temperature, which when combined with the z value measured at $T_g(H)$ gives a ν of 1.1±0.2. This agrees reasonably well with the value reported by Koch *et al.* of 1.7 and Gammel, Schneemeyer, and Bishop of 2±1. This interpretation of the ohmic resistance is strong evidence for point 2.

Below the transition, the voltage vanishes quickly making accurate measurement of the E-J curves, over the region in current density where the scaling is expected, difficult and we have been unable to extract a value of the exponent μ. However, a scaling collapse of the E-J data

suggested by Koch, Foglietti, and Fisher,[21] shown in Fig. 7, indicates that the same critical exponent ν applies to the data above and below the phase transition. In Fig. 7 we plot E/J scaled by $|t|^{\nu(z-1)}$ versus J scaled by $|t|^{2\nu}$ for two fields 0.3 and 1.5 T for sample A [Fig. 7(a)] and sample B [Fig. 7(b)]. This scaling form allows the data from all the E-J curves at different temperatures and fields to be combined. The two branches represent the universal scaling functions.[13] Also, finding that this scaling collapses the data for both fields demonstrates the universality of the critical exponents ν and z for the two fields and samples. The fact that the same value of ν collapses both the data above and below $T_g(H)$ demonstrates support for the third vortex-glass prediction listed above.

It is clear that the scaling collapse for sample A is better than for sample B. This may partly be due to the fact that sample B has larger grains. Equation (2) can be used to estimate the maximum current density where critical scaling should be observed. Sample A (5-μm grains) has a glass transition temperature of 55 K at 1.5 T. This implies that above 15 000 A/m^2 critical scaling should not be observed. For sample B (8-μm grains) the glass temperature is 67 K at 1.5 T which implies a limit of 7000 A/m^2. Figure 8 shows the E-J data at T_g where E has been scaled by $I^{(z+1)/2}$. This scaling makes the

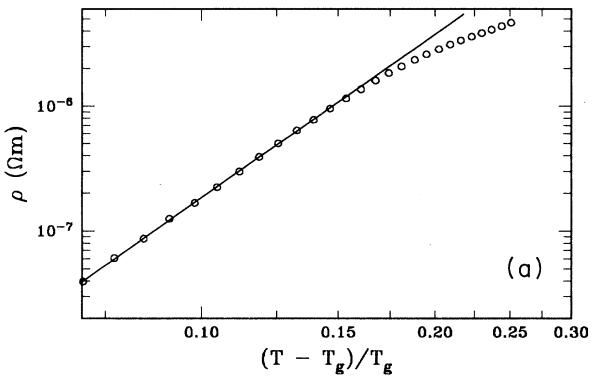

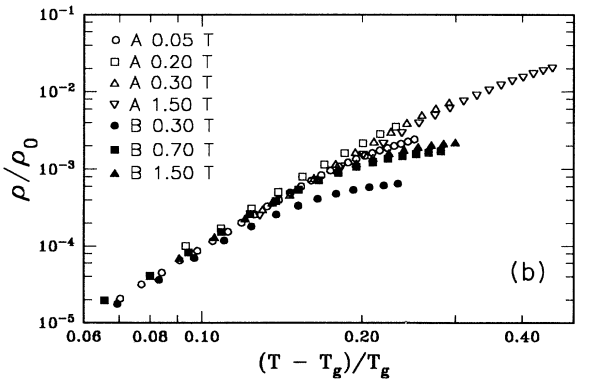

FIG. 6. (a) The resistivity in the ohmic region above T_g vs $(T-T_g)/T_g$ for sample A at an applied field of 0.05 T. The fitted curve has a slope of 4.2. (b) The resistivity in the ohmic region above $T_g(H)$ divided by $\rho_0(H)$ vs $(T-T_g)/T_g$ for several fields for both samples.

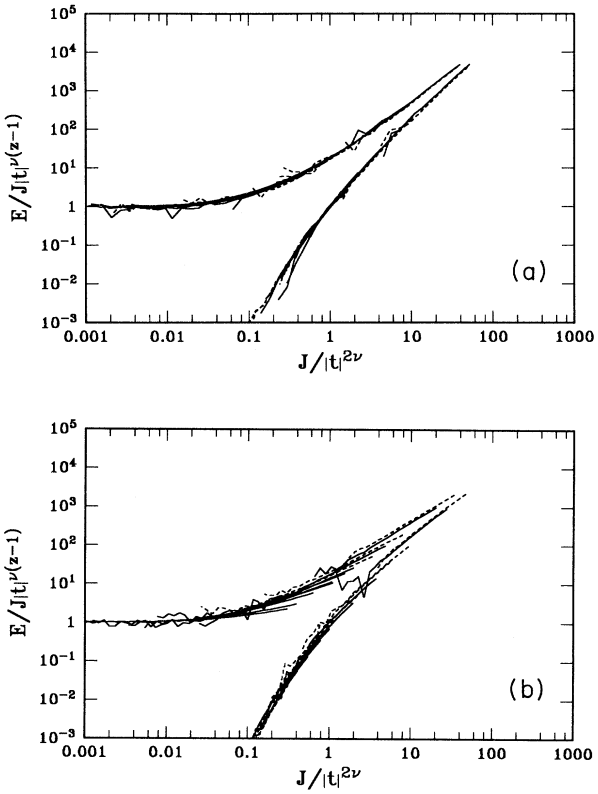

FIG. 7. (a) Sample A, $E/J|t|^{\nu(z-1)}$ vs $J/|t|^{2\nu}$ for 0.3 and 1.5 T. (b) Similar data for sample B. For both plots, $z=4.6\nu=1.1$.

critical region appear as a constant. We have estimated the current where the deviation from scaling behavior is a factor of 2. The difference between the two samples is consistent with the factor $\frac{15}{7}$ estimated above. The magnitude of the current density where deviation from scaling is observed is also in very good agreement. This grain

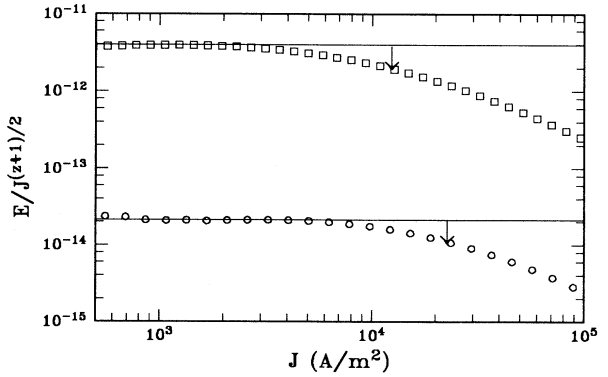

FIG. 8. $E/J^{(z+1)/2}$ vs J for the value of T closest to the glass temperature at 1.5 T. The data for sample B are plotted as squares and sample A as circles.

size dependence provides a very strong argument in support of the vortex-glass model, however, it also, when combined with the experimental constraints of noise, reduces the amount of data for sample B. The effect of the different grain size is also evident in the size of the critical region in Fig. 5(b). The solid points, from sample B, clearly diverge from the expected scaling behavior at a smaller value of reduced temperature than the open points from sample A. The coherence length of the fluctuations diverges as the glass transition is approached along the temperature axis. For the predicted scaling behavior to be observed, this length must be larger than any other relevant length in the sample, i.e., the grain size in polycrystalline material. Because sample B has larger grains, a smaller value of reduced temperature is necessary before this condition is met.

Collective pinning[12] models also predict zero linear dissipation, however, the assumption in the collective pinning model that large numbers of random pins induce small local distortion of the hexagonal flux lattice does not seem appropriate for polycrystalline samples. The models based on transitions in a flux liquid regime[13] also do not appear appropriate. They predict that entanglement or partially ordered flux lattice phases could provide the rigidity necessary to support a critical current. However, these models, which are probably more relevant at very low-flux density, have not been developed to the point where detailed comparisons with transport data such as reported here are possible.

We have presented transport data on two polycrystalline $YBa_2Cu_3O_{7-x}$ samples which strongly support the conclusion that there exists a global second-order phase transition where the vortices in the intergranular regions freeze into a state with true superconducting character. This phase can only be detected when the measurement current density is small enough to probe the sample at lengths larger than the average grain size. The critical exponents measured at this transition are in very good agreement with those measured for epitaxial films[15] and crystals[16] of $YBa_2Cu_3O_{7-x}$ and are consistent with the preliminary predictions of Fisher's[14] vortex-glass model.

ACKNOWLEDGMENTS

We are grateful for a very productive collaboration with M. P. A. Fisher and his colleagues, D. S. Fisher and D. A. Huse. We also acknowledge helpful conversations with R. H. Koch and A. P. Malozemoff. We are appreciative of the work of P. R. Duncombe in sample preparation. This work was supported in part by the Defense Advanced Research Project Agency (DARPA) under Contract No. N00014-89-C-0112.

---

*Present address: Department of Materials Science and Engineering, Cornell University, Ithaca, NY 14853-1501.

†Present address: Materials Department, University of California at Santa Barbara, Santa Barbara, CA 93106.

[1]P. W. Anderson, Phys. Rev. Lett. **9**, 309 (1962).

[2]Y. B. Kim, C. F. Hempstead, and A. R. Strand, Phys. Rev. Lett. **9**, 306 (1962).

[3]M. R. Beasley, R. Labusch, and W. W. Webb, Phys. Rev. **181**, 682 (1969).

[4]J. M. A. Wade, Philos. Mag. **20**, 1107 (1969).

[5]J. E. Nicholson, B. S. Cort, and G. P. Cort, J. Low Temp. Phys. **26**, 69 (1977).

[6]K. A. Müller, M. Takashige, and J. G. Bednorz, Phys. Rev. Lett. **58**, 1143 (1987).

[7]C. Ebner and A. Stroud, Phys. Rev. B **31**, 165 (1985).

[8]T. K. Worthington, W. J. Gallagher, T. R. Dinger, and R. L. Sandstrom, in *Novel Superconductivity,* edited by S. A. Wolf and V. Z. Kresin (Plenum, New York, 1987), p. 781.

[9]A. P. Malozemoff, in *Physical Properties of High Temperature Superconductors,* edited by D. Ginsberg (World Scientific, Singapore, 1989), p. 71.

[10]A. P. Malozemoff, T. K. Worthington, R. M. Yandrofski, and Y. Yeshurun, in *Towards the Theoretical Understanding of High Temperature Superconductivity,* edited by S. Lundqvist, E. Tosatti, M. Tosi, and Y. Lu (World Scientific, Singapore, 1988); C. W. Hagen and R. Griessen, Phys. Rev. Lett. **62**, 2857 (1989).

[11]E. Zeldov, N. M. Amer, G. Koren, A. Gupta, M. W. McElfresh, and R. J. Gambino, Appl. Phys. Lett. **56**, 680 (1990).

[12]M. V. Feigl'man, V. B. Geshkenbein, A. I. Larkin, and V. M. Vinokur, Phys. Rev. Lett. **62**, 2857 (1989).

[13]D. R. Nelson and H. S. Seung, Phys. Rev. B **39**, 9153 (1989); M. C. Marchetti and D. R. Nelson, *ibid.* **41**, 1919 (1990); S. P. Obukhov and M. Rubinstein, Phys. Rev. Lett. **65**, 1279 (1990).

[14]M. P. A. Fisher, Phys. Rev. Lett. **62**, 1415 (1989); D. S. Fisher, M. P. A. Fisher, and D. A. Huse, Phys. Rev. B **43**, 130 (1991).

[15]R. H. Koch, V. Foglietti, W. J. Gallagher, G. Koren, A. Gupta, and M. P. A. Fisher, Phys. Rev. Lett. **63**, 1511 (1989).

[16]P. L. Gammel, L. F. Schneemeyer, and D. J. Bishop Phys. Rev. Lett. **66**, 953 (1991).

[17]T. M. Shaw, D. Dimos, P. E. Batson, A. G. Schrott, D. R. Clarke, and P. R. Duncombe, J. Mater. Res. **5**, 1176 (1990).

[18]J. E. Evetts and B. A. Glowacki, Cryogenics **28**, 641 (1988); J. W. Ekin, Appl. Phys. Lett. **55**, 905 (1989); J. E. Evetts, B. A. Glowacki, P. L. Sampson, M. G. Blamire, N. McN. Alford, and M. A. Harmer, IEEE Trans. Magn. **25**, 2041 (1989).

[19]Y. Yeshurun and A. P. Malozemoff, Phys. Rev. Lett. **60**, 2202 (1988).

[20]M. Tinkham, Phys. Rev. Lett. **61**, 1658 (1988).

[21]R. H. Koch, V. Foglietti, and M. P. A. Fisher, Phys. Rev. Lett. **64**, 2586 (1990).

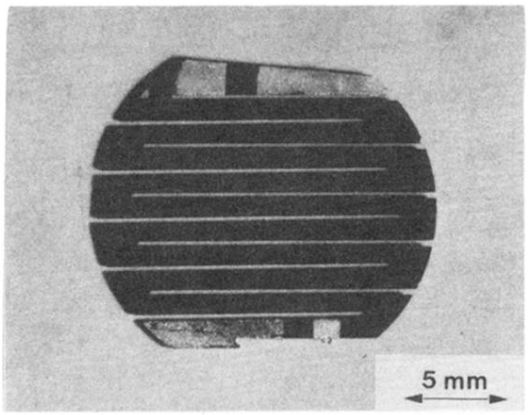

FIG. 1. A photograph showing the serpentine pattern used to achieve large electric field sensitivity.